Simulated Hybrid Off-grid System Configurations Based on Linear Optimized Method in Cairo International Airport

Alaa Emad[1], Mahmud Omer[2], Adham Osama[3], Mohamed Tarek [4]

1: Ph.D. student, Khalifa University, Department of Electrical and Computer Engineering, Abudhabi

2: Research Associate, Khalifa University, Department of Electrical and Computer Engineering, Abudhabi

3: MSc Student, Khalifa University, Department of Electrical and Computer Engineering, Abudhabi

4: Ph.D. Student, Khalifa University, Department of Electrical and Computer Engineering, Abudhabi

***Abstract*— The integration of various renewable resources has been excessively studied and investigated to form a reliable energy system. This system will be used to sustain the load requirements maintaining energy consumption rates. In this paper, a Hybrid off-grid system of different configurations have been studied to investigate the effect of each renewable resource in maintaining the energy balance of the system. Furthermore, this study aims to find the appropriate configuration of the hybrid system structure for the studied site. A new method named "Deterministic Balanced Method" was introduced based on the integration of power ratings of the system components to get the total annual energy production for the project lifetime. This method is used in comparison with the results of other software tools such as HOMER. Then, verification of the sizing optimization results for the conducted methods is achieved by comparing the power ratings and annual energy production. This paper has also included a real case study of the hybrid renewable energy generation systems in the Cairo International Airport after considering the amount of solar radiation and wind speed collected by international weather data platforms such as NASA and METEONMRM. This system design was also based on an actual load studied and represented to ensure the feasibility of this study. Finally, Simulink was investigated to ensure energy storage system optimization.**

Keywords—Energy Systems, Hybrid, off-grid, Solar PV, Wind turbines, hydrogen system.

I. INTRODUCTION

A hybrid mix of photovoltaic generators, wind turbine generators, and energy storage elements are the most pandemic mix of energy production in many studies and scientific research [1]. The advantage of each component used in the system is fully utilized and overrides the merits of other generation components. This paper has discussed three cases showing different renewable energy penetration percentages for WTGs and PVs. The adverse nature of the wind-PV system can compensate for the intermittency nature of each system and, therefore, improve the hybrid system's overall reliability [2]. Different hybrid system configurations can be implemented in the studied site. However, there are crucial points of comparison that will be discussed throughout the paper, which will drive the proposed system to be physically accepted in terms of feasibility and economy. In this paper, solar PV, wind turbines, fuel cells, and electrolyzer are sized and utilized to serve the community load.

Research conducted by [3] discussing the potential for hydrogen in the marine environment, showing up the current state of transferable technologies and the technical and economic issues that need to be addressed in the context of the ship design. The study mainly focused on setting up a hybrid system for electricity and hydrogen production and reducing the greenhouse emissions produced from the industrial processes. The hydrogen marine system proposed here uses natural gas (NG) as its base feed to produce LH_2 in the fuel plants located in the container terminals at each end of the three routes considered. Another research carried by [4] described the design information of solar PV and wind turbine hybrid power generation system to provide electricity to a model community of 100 households and health clinic and elementary school. The optimal simulation results in this study showed that PV/wind turbine/diesel generator/battery and convertor is the best-configured system for their application with a renewable fraction of 84%. These given numbers were used to give a rough estimate for the previous research works focusing on the renewable resources' penetration (increasing the renewable fraction percentage) and to select the best configuration for the application targets. Many research papers and publications introduced different system configurations and comparative analysis to decide the most economically feasible one. One of those researches was the paper presented by [5] for a case study in the desert region of the United Arab of Emirates. It presented a technical-economic analysis based on integrated modeling, simulation, and optimization approach to design an off-grid hybrid solar PV/Fuel Cell power system. This system was designed to meet the energy demand of 4500 kWh/day of the residential community (150 houses). The total power production from the distributed hybrid energy system was 52% from the solar PV and 48% from the fuel cell, with a 40.2 % renewable fraction which is considered a low value for renewable energy penetration of this system. Consequently, one of the main concerns of the paper research was to achieve a renewable fraction of 100% in the simulated configurations of various hybrid off-grid systems.

The main grid is usually connected to the Distribution Network Operator (DNO) from which various microgrids emerge. A typical microgrid consists of AC loads, DC loads, Battery Energy Storage Systems (BESS), wind generators, solar generators, and diesel generators [6]. The AC/DC microgrid can be configured in various ways. In the first

configuration, all the generators, BESS, and AC loads are connected to a single DC bus. The AC power from the wind and diesel generators is converted into DC before it is fed to the DC bus. Also, the DC power from the DC bus is converted to AC power before it is utilized in the AC loads. In the second configuration, all the entities are connected to two AC and DC buses with a single DC/AC converter, while the third configuration has two DC/AC converters. In both scenarios, power from the AC bus is converted to the DC before it is fed to the DC bus, and vice versa [7] [8]. Essentially, this forms the basis of the distributed hybrid network, as suggested by Mohamed et al. in their study [1]. The researchers propose a hybrid network comprising a hub system, AC/DC microgrid, electrical grid, electric vehicles, and AC and DC loads. Using the PDMM technique, the researchers observed an optimal power transaction between the hybrid and AC/DC networks. Besides, the researchers established that the unscented transformation (UT) method could effectively forecast errors in the system based on the correlation among the various uncertainty parameters.

According to Ortiz et al., when designing an appropriate configuration, it is necessary to consider the power reliability, observability, economy, controllability, and flexibility based on the principles of power quality assurance, partition, and hierarchy while maximizing the use of resources [9]. Based on these principles, the researchers proposed and designed a microgrid that was divided into three: two AC and one DC microgrid. The entire system consisted of the main grid, medium voltage, low voltage, and DC voltage. The microgrid had a non-linear load. The DC bus comprised the photovoltaic (PV) system, BES systems, AC/DC, and DC/DC converters. The study explored two main scenarios: the maximum and minimum power demands. The peak solar radiation coincides with the maximum demand period for the solar generators, which occurs at 11h00. The researchers established that in the maximum demand, the average deviation of the maximum deviation was 0.046 per unit, and positive results are observed in all the buses for the minimum demand. In the power balance scenario, in each bus, power decreases during maximum demand when only the diesel generator is connected. However, active power losses are observed in each phase due to the unbalanced load. The maximum loss per phase is less than 1.4kW, which is comparatively low compared to the loss during the maximum demand [9]. Overall, the distributed grid (DG) can help reduce the overdependence on fossil fuels and enhance the efficiency of the electrical grid, especially when connected to the smart grid.

The optimization techniques used for the hybrid systems is complex as it requires the detailed model of each component used, where it can be used to target a specific objective. For example, figuring out the rated components of the hybrid system to get the least net present cost. optimal sizing of the hybrid system can be classified into three main categories:

- Basic technical methods such as the Energy balance method
- simulation programs such as HOMER, HYBRID 2, and HOGA programs
- metaheuristic optimization algorithms such as particle swarm optimization (PSO), tabu search (TS), simulated annealing (SA), harmony search (HS), and Genetic Algorithm (GA)

An objective function must be defined for any optimization method, and it can be single or multi-objective functions depending on the technical terms it optimizes [64]. In this system model, there are two main objective functions:

These equations can be solved using any of the methods mentioned in Figures (1,2) as there are two main optimization algorithms for solving this. Firstly, the deterministic method, which is efficient on a unimodal search landscape, Reliable in finding the same solution and has a low computational cost. However, it has certain limitations and drawbacks as it has a high dependency on the initial solution and a slow rate of convergence to the real solution. Lastly, the second method is the stochastic method, which performs well in unimodal and multimodal search space landscapes and has low dependency on the initial solution. Even though stochastic methods have a slow convergence speed and find a different answer in each run, they are most commonly used to solve multi-objective functions [10]. In this thesis, the deterministic iterative balance method is used to solve the proposed model's objective functions and achieve the optimized solution concerning all constraints.

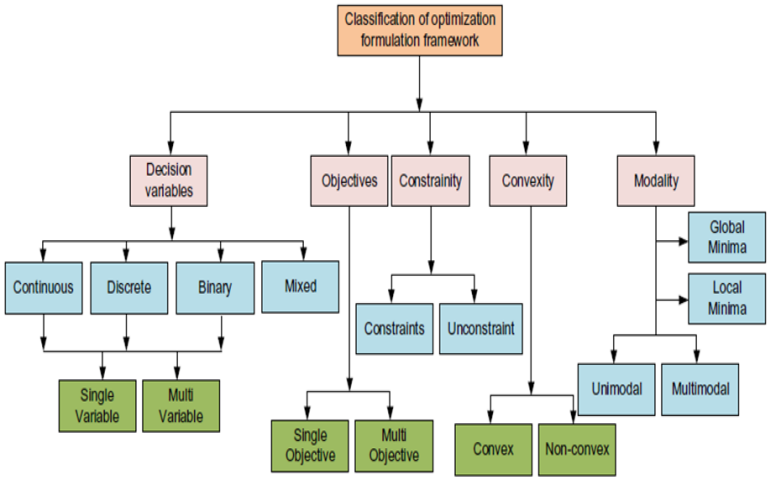

Figure 1.Optimization Methodology [10]

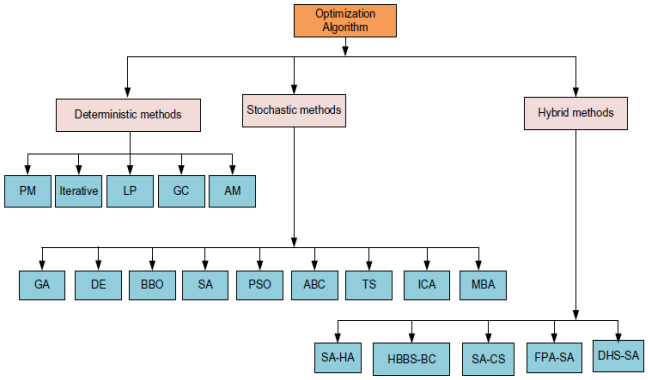

Figure 2. Optimization Techniques [10]

This brief overview of the proposed hybrid off-grid systems in industry and research agencies concludes that the proposed system in this thesis must follow specific outlines that are mandatory to design an energy hub for electricity and fuel production. This system is considered to achieve a 100% renewable fraction with different system configurations as follows (PV/WTG/ELZ/FC)-(WTG/FC/ELZ)-(PV/ELZ/FC).

II. MODDELING SYSTEM COMPONENTS

1. Photovoltaic Arrays

The main objective functions were used to get the output power of the PV modules taking into consideration the efficiency of the modules and other derating factors. The first equation used in PV modeling is an output power function of Irradiance [11].

$$P_{pv} = Y_{pv} f_{pv} \left(\frac{G_T(t)}{G_{T,STC}} \right) \qquad (1)$$

Other factors that had been encountered during the literature view. Temperature and wind speed had significantly affected the model to get more accurate results that are feasible for execution. Consequently, another objective function for calculating the output power was then evolved, providing a relation between the Irradiance and temperature to deliver the actual output power shown in equation [12]:

$$p = \eta T_{ref} A G_T [1 - 0.0045(T_c - 298.15)] \qquad (2)$$

After studying the behavior of temperature and Irradiance throughout the meteorological model, the effect of this behavior was linked to the changes in each of the two parameters and the overall efficiency of the PV system [7]. This relation was supported by the following equation:

$$\eta = \eta_{Tref} [1 - B_{ref} (T_{c,i} - T_{ref})] \qquad (3)$$

Fig. (3) shows the effect of temperature on the produced output power, where the efficiency decreases with the increase in temperature resulting in power reduction. However, solar modules' energy production, considering the temperature effect increases in mild atmosphere countries like Egypt as shown in Fig.4.

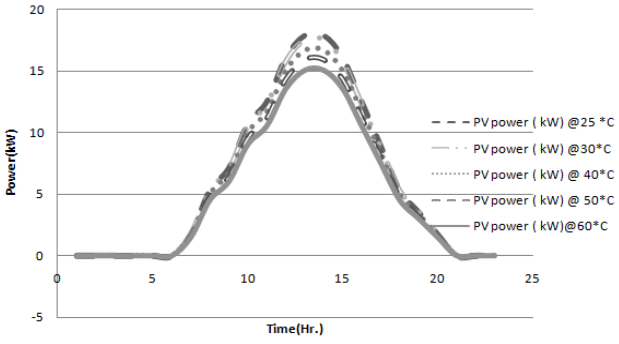

Figure 3. Effect of temperature on the output power of PV

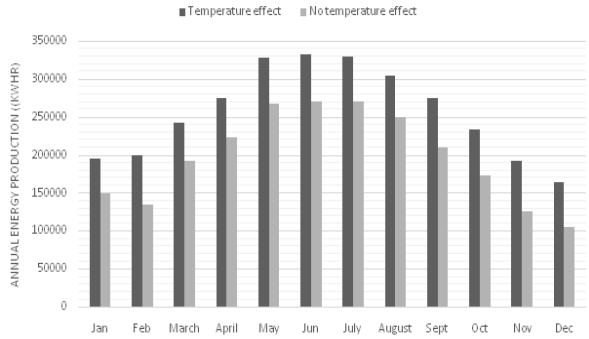

Figure 4. Effect of temperature on monthly energy production in Cairo

2- Wind Turbine Generators (WTGs)

The Wind Turbine Generator (WTG) hourly power output at the studied location depends on the hourly wind speed, as shown in Fig.3. It can be expressed by the following equations [13]:

$$P_{wind}(V_V) = \begin{cases} P_r(A + BV_V + CV_V{}^2), & V_D \le V_V \le V_N \\ P_r, & V_N \le V_V \le V_R \\ 0 & Elsewhere \end{cases} \qquad (4)$$

Where:

V_N is the Rated speed (m/s), V_D Cut-in speed (m/s), V_R is Cut-off speed (m/s), V_V is Wind speed (m/s), P_{wind} is Power of wind generator (W), P_r is Rated electrical power output (W). Generally, the cut-in speed of a wind turbine is in the range of2.5-3.5 m/s, and the cut-out speed is in the range of 20-25 m/s.

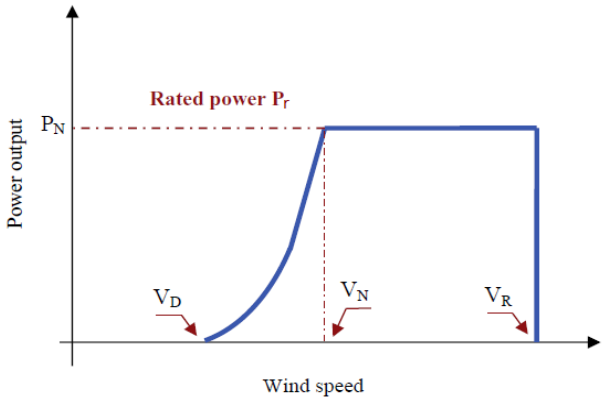

Figure 5. Power output curve of wind turbines

3. Hydrogen System

A fuel cell can be defined as an electrochemical device that produces electrical power directly from a fuel like hydrogen, natural gas, diesel, and propane. Its operation is similar to that of a conventional battery except in some parts that will be discussed in detail later in this paper and will affect the modeling of the hybrid off-grid system. Accordingly, their development has been much related to the development of electrochemistry more than power engineering, and it is already studied as a distinct branch of physical chemistry [14].

The second element in the hydrogen system is the electrolyzer, an electrochemical device that creates electrolysis for the water molecules to produce hydrogen and oxygen. This process is powered by the excess electrically in the system. In other words, an electrolyzer is used to convert the unused electrical energy into stored chemical energy inside hydrogen and then recall it back in the time of operation. The mathematical formula of the produced hydrogen from the electrolyzer can be expressed as follows [15]:

The energy required to produce one kilogram of hydrogen

$$= \eta_{Elz} X \frac{H_2 Heating\ Value}{H_2 density} \qquad (5)$$

$$\text{Hydrogen produced in kilograms} = \frac{P_{Elz}}{Energy\ required\ to\ produce\ one\ kilogram\ of\ hydrogen} \quad (6)$$

A hydrogen tank is also used for hydrogen storage, where it acts as a device used to store either compressed hydrogen gas or liquid at a certain pressure and limited capacity. Hydrogen tanks are usually equipped with protection devices like pressure relief. The specs of the hydrogen tanks are mainly dependent on the nature of the application (for example, fuel cell electric vehicles, generating electricity, cement production).

4. Control System

As shown in Fig. 6, the control system is used for this studied structure in controlling the switching operations of the hydrogen system. Considering the hydrogen tank level, available surplus power, and power deficit, the controllers operate the electrolyzer and fuel cell and report system alarms using SCADA HMI on failure cases of sustaining the energy balance between generation and demand side.

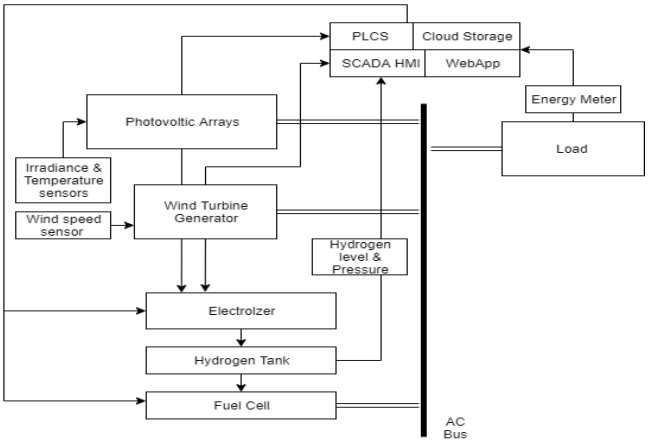

Figure 6. Power Management System

III. Hydrogen System Analogy with Battery Storage System

The main difference between the hydrogen storage and battery storage systems, as shown in Fig.(7,8), is their efficiencies during charging and discharging. It was found that the battery system has an advantage over that hydrogen system that efficiency during the charging and discharging modes are almost the same, unlike the hydrogen system where efficiencies of the electrolyzer and hydrogen pump are determining the charging efficiency. The efficiency of the fuel cell is what controls the discharging efficiency. However, this paper used the hydrogen system as the primary energy storage element because of its energy storage capacity and the flexibility to store surplus energy and share it with other energy systems.

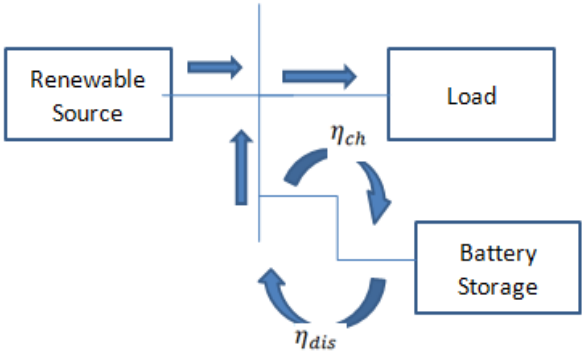

Figure 7. Charging and discharging in the Battery system

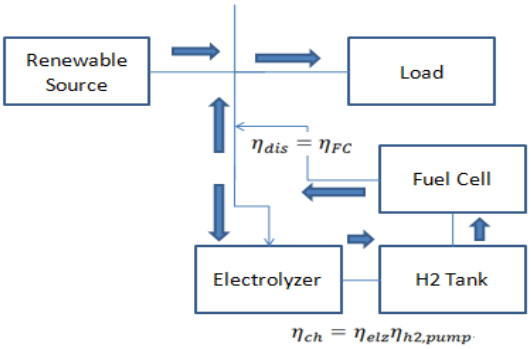

Figure 8. Charging and discharging in a hydrogen system

After studying and modeling the proposed hybrid off-grid system components and based on the available commercial datasheets, system design standard ratings were chosen as shown in Table I and used in the methodology of sizing optimization of the different topologies of the system.

TABLE I. SYSTEM POWER RATINGS

Photovoltaic Modules		**Wind Turbine**	
Panel peak power (kW)	0.335	Rated Power (kW)	660
Number of panels	1180-4375	Cut in/out wind speed (m/s)	3.0/25.0
Panel area(m2)	1.6	Rated wind speed	15
Solar cell material	Monocrystalline Maxeon GEN III	Power density (w/m2)	380.4 W/m2
Manufacturer	Sun Power	Manufacturer	Vestas
Model	SPR-X21-335-BLK	Model	V47-Onshore
Efficiency (%)	21	Hub-height(m)	40/45/50/55
Fuel Cell		**Electrolyzer**	
Nominal Power	250 kW	Nominal Power	300 kW
H2 consumption rate	5800 Btu/kWhr	H2 production rate	60 Nm3/hr
Input Pressure	15 psig	Output pressure	10 barg-27barg
AC Power Production	5 kWhr/Nm3	AC power consumption	5 kWhr/Nm3
Nominal efficiency	90%	Nominal efficiency	80%
Manufacturer	ES5-EA2AAN	Manufacturer	Hydrogenics
Model	Bloom Energy	Model	HySTAT-60-10

IV. Load Profile

This study assumes that the DC and AC wiring losses are small enough to be neglected due to the small geographic scatter of the study system. (USA_AK_Anchorage.Intl.AP.702730_TMY3_BASE) the load profile is used in this study [16], and the peak load is set to 250 kW. The load profile is then determined per hour for the 8760 hours of a year.

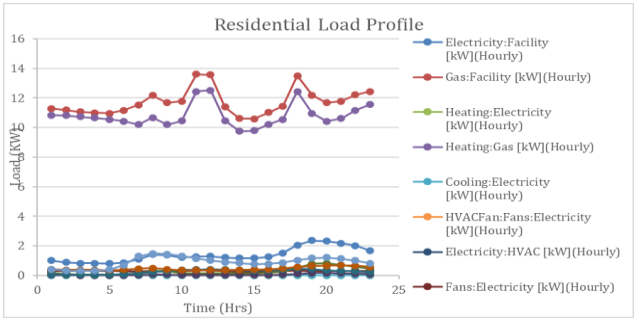

Figure 9. Residential Load profile

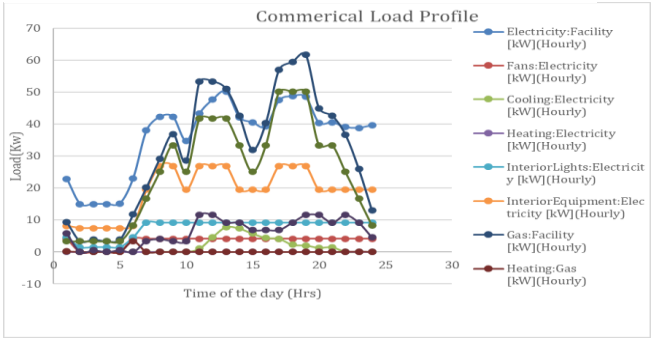

Figure 10. Commercial Load Profile

V. Meteorological Data

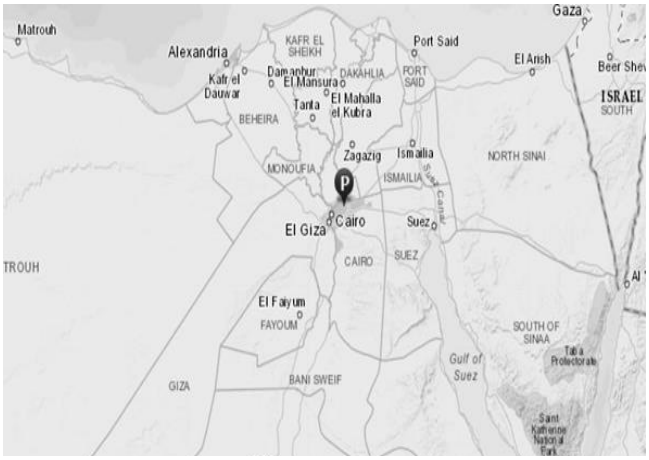

Figure 11. Site of the meteorological model at Cairo International Airport [12]

VI. Methodology

Three different configurations were conducted for the hybrid off-grid system structure as follows a) Solar PV / hydrogen system b) WTG/hydrogen system c) PV/WTG/Hydrogen system. Those different systems were chosen to apply the deterministic balance method to achieve the optimal sizing and cost analysis for the studied location. The methodology of this method was based on selecting the critical month for lack of energy for system design and then making the surplus power production of the Solar PV or WTGs equal to the load demand plus system losses in times of non-renewable

METEONORM7.1 Version was used in the analysis phase of computing meteorological data in 30.083 Latitudes, 31.283 Longitude at an altitude of 36 m. This location was selected because of the limited available stations available in the METEONORM database as there were only two locations in Cairo with a detailed meteorological model. METEONORM database is a powerful tool for having total Irradiance, temperature, wind speed profiles at any time step and during any day of the year. It also offers unique access to the Global Energy Balance Archive Data (GEBA) [17]. The periods 1981-1990 and 1991-2010 are available for solar irradiation on a global scale used to get the input files of Irradiance and temperature and wind speed (8760 values in a time step of one hour during the whole year). The uncertainty of the database and the generated typical years is transparently shown directly in the software.

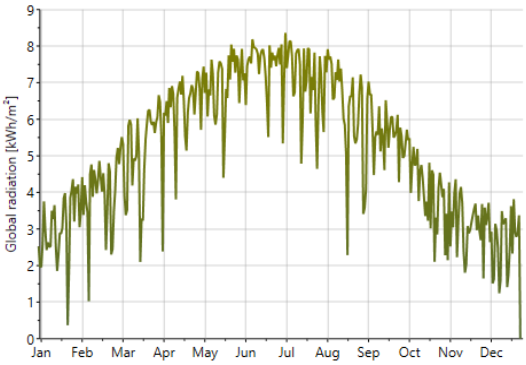

Figure 12. Global Irradiance during the year [12]

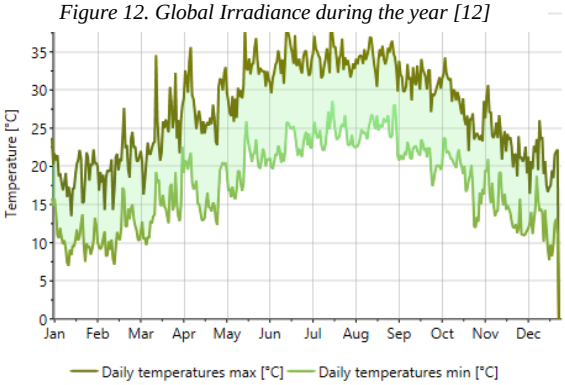

Figure 13. Temperature profile during the year [12]

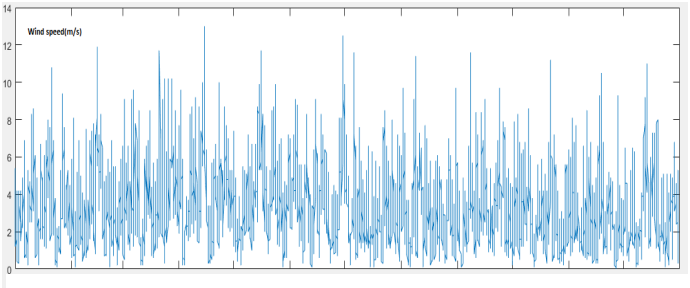

Figure 14. Wind speed profile using METEONORM

generation ($E^{+}= E^{-} + sys_{losses.}$) as shown in Fig.13 where E^{+} : Surplus energy supplied by PV arrays/ WTGs, E^{-} : Total lack of energy which will be supplied by the fuel cell and electrolyzer, E_D: Energy demanded by load and supplied by PV arrays/WTGs. This method is known as the deterministic balance method (DBM). December was chosen to be the month of study for selecting the irradiance profile, temperature ranges, and sun duration hours for the Solar PV system. The critical limit of system design was deduced based on powering a load at its maximum demand in a day of low Irradiance. This case represents the worst-case scenario that the system could face during the year. For the standalone wind system, the meteorological data indicated that November would have very low wind speeds for the studied site, making the system generate electricity for several days. Consequently, the system power ratings were deduced after several iterations for satisfying the energy balance in these critical months of design, as shown in Fig.16.

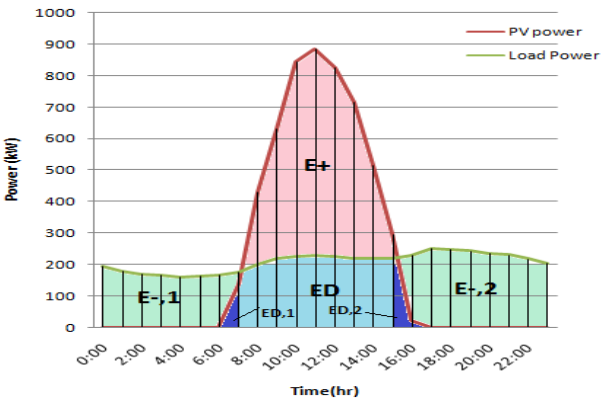

Figure 15. Energy profile for solar PV standalone system

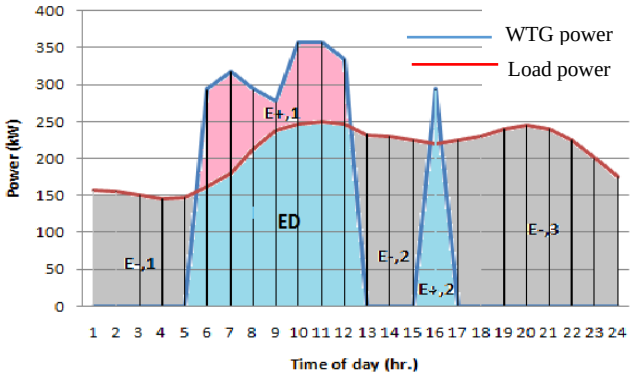

Figure 16. Energy profile for standalone Wind system

VII. Results & Discussion

The results for each system topology were illustrated in Fig. (17,18,19). To check that the system design was not overestimated or underestimated, the critical month of design is expected to be the month of no excess energy generation as the system is optimally designed to meet the load. After running several iterations to achieve the energy balance in the selected month, the installed capacities for Solar PV, fuel cell, and electrolyzer are 1793 kW, 300 kW, and 800 kW, respectively, in a standalone solar system. For wind/hydrogen systems, Wind turbines, fuel cells, and electrolyzer are 1340kW, 300 kW, and 800 kW, respectively. For hybrid solar/wind, solar PV 1466 kW, WTGs are 250 kW, fuel cell 300 kW, and electrolyzer 800 kW. Those system configurations were based on 100% renewable fraction with no greenhouse emissions and sustaining energy balance in critical cases for energy lack during the year. The annual energy production for the three systems are 2,455,387: 2,901,427: 3,377,699 respectively meeting a community load profile of average 1,817,700 kWhr/year. The excess energy production for this year was recommended to be exported to the grid or shared with other energy storage systems.

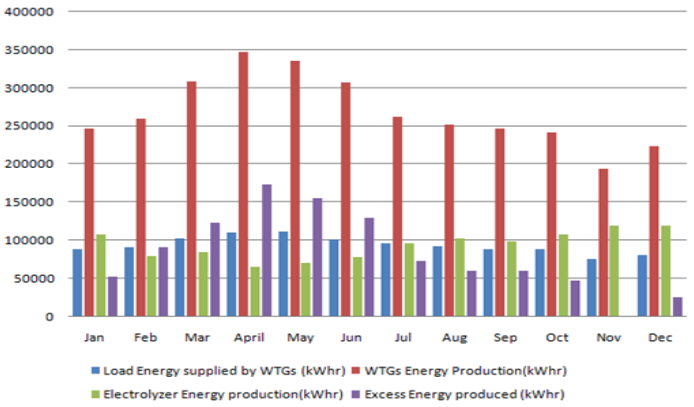

Figure 17. Energy production profile for standalone solar PV system

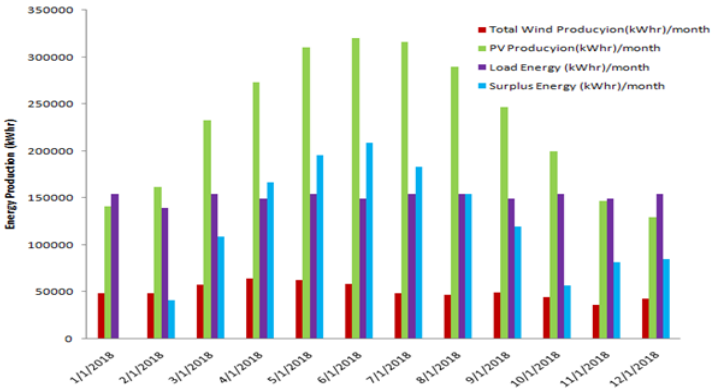

Figure 18. Energy production profile for standalone wind system

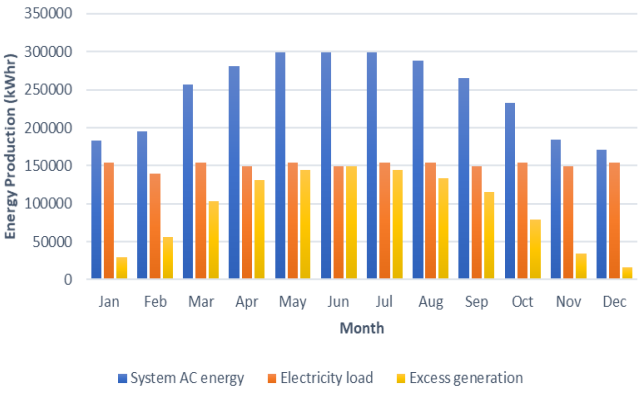

Figure 19. Energy production profile for hybrid solar PV/wind system

VIII. COST ANALYSIS

The cost objective function was elaborated where the cost sheet in Table I is directly substituted, and DBM is applied in minimizing the function and obtaining the optimum configuration resulting in the least total annualized cost. To optimally design the hybrid generation system, the optimization problem, defined by Eq. (9), must be solved.

$$C_{cpt} = \frac{i(i+1)^n}{(1+i)^n-1}[N_{pv}\ X\ C_{PV} + N_{WTG}\ X\ C_{WTG} \\ N_{Tank} X\ C_{Tank} + C_{FC/ELZ} + N_{conv} X\ C_{conv}] \quad (7)$$

C_{PV} is the unit cost of the PV panel, C_{WTG} is the unit cost of the wind turbine generator, N_{tank} is the number of storage tanks, C_{Tank} is the unit cost of the hydrogen storage tank, and $N_{Conv/Invis}$ the number of converter/inverter systems.

$$C_{Mtn} = N_{PV} X\ C_{PV,Mtn} + C_{FC,Mtn} + C_{Elz,Mtn} \\ + N_{WTG}\ X\ C_{WTG,Mtn} \quad (8)$$

Where $C_{PV.Mtn}$, $C_{WTG.Mtn}$, $C_{FC,Mtn,}$ and $C_{Elz,Mtn}$ are the annual maintenance costs of PV, wind turbines, fuel cell, and electrolyzer systems, respectively.

To minimize the total cost function,

$$C_T = C_{cpt} + \quad C_{Mtn} \quad (9)$$

For the PV/ Wind/ hydrogen hybrid system, the following constraints should be satisfied:

N_{PV}=Integer, $N_{Min,PV} \le N_{PV} \le N_{Max,PV}$ (10)
N_{Wind}=Integer, $N_{Min,wind} \le N_{wind} \le N_{Max,wind}$ (11)
N_{FC}=Integer, $N_{Min,FC} \le N_{FC} \le N_{Max,FC}$ (12)
N_{Tank}=Integer, $N_{Min,Tank} \le N_{Tank} \le N_{Max,Tank}$ (13)
$N_{Converter/Inverter}$=Integer, $N_{Min,Conv./Inver} \le N_{Conv./Inver.} \le N_{Max,Conv./Inver}$ (14)

The deterministic method used here is efficient on a unimodal search landscape, reliable in finding the same solution, and has a low computational cost. However, it has certain limitations and drawbacks as it has a high dependency on the initial solution and a slow rate of convergence to the real solution. Additionally, LCOE is an indicator of the price of electricity for every one kW-hr after considering the discount rate and inflation rates for the project lifetime. This indicator does not include any government incentives or financial support.

$$LCOE = \frac{Total\ Life\ Cycle\ Costs\ (TLCC)}{Total\ Lifetime\ Energy\ Production} \quad (15)$$

The Levelized Cost of energy is crucial for determining the feasibility of the designed system and how it could be scaled to satisfy the end user's demand fully by reviewing different international references offered by renewable energy centers like IRENA, REN21, RCREEE, World bank. It can be deduced that the energy mix adopting renewable energy resources is a strategic vision. Analyzing the trends in the LCOE of projects being executed globally, it was suggested that the average LCOE for solar PV is in the range of USD 0.06/KWh by 2019, which is slightly expensive than onshore wind at USD 0.05/kWh [18]

IX. HOMER PRO SIMULATION RESULTS

HOMER -Pro [19] is an optimization model which performs thousands of simulations and gives the best possible techno-economic design for the system. Solar PV/hydrogen-WTG/Hydrogen - Solar PV/WTG/Hydrogen configurations were set by switching components as shown in Fig. 18 and simulated at the site of Cairo International Airport. The load profile was imported into the program for one year, and the results for the different simulated topologies as shown in Table II.

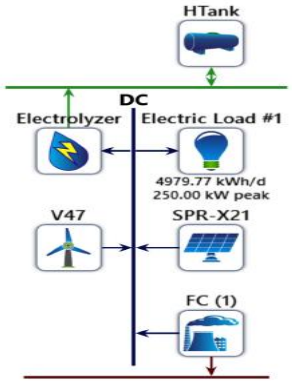

Figure 20. HOMER PRO Model [19]

TABLE II. HYBRID SYSTEM CONFIGURATIONS COMPARISON

Point of Comparison	PV/FC/ELZ	WIND/FC/ELZ	PV/WIND/FC/ELZ
Energy Production using DBM (kWhr)	2,905,172	3,223,807	3,377,699
Energy Production using HOMER (kWhr)	3,138,000	3,696,359	3,262,563
Absolute difference (%)	-5%	-14.5%	+3.5%
Energy Production using SAM (kWhr)	2,954,031	-	-
Installed Capacity using DBM (kW)	PV: 1793 kW FC: 300 kW ELZ:800 kW H2 tank: 100 kg	WTG: 1340 kW FC:300 kW ELZ:1000 kW H2 tank: 100 kg	PV: 1466 kW WTG: 250 KW FC: 300 kW ELZ:800 kW H2 tank: 100 kg (best economic config.)
Installed Capacity using HOMER	PV: 1803 kW FC: 200 Kw ELZ:400 kW H2 tank:100 kg	WTG: 1980 kW FC:200 kW ELZ:500 kW H2 tank:150 kg	PV:1032 kW WTG:1320 kW FC:250 kW ELZ:500 KW H2 tank:150 kg
Levelized cost of energy-DBM	$0.247	$0.237	$0.211
Levelized cost of energy-HOMER	$0.332	$0.310	$0.232
Control Algorithm	DBM	DBM	DBM/Fuzzy logic
Greenhouse emissions	Only manufacturing material	Only manufacturing material	Only manufacturing material

To solve the issue of overproduction in some periods during the steady-state operation. MATLAB/Simulink model was introduced for a dynamic behavior and how optimization techniques can be managed for energy storage systems like batteries and hydrogen systems, as shown in the figure below.

Linear Program-Based Optimization
The standard form of the linear program (LP) -Linprog

Min $f^T x$ such that $\begin{cases} A.X < b \\ A_{eq}.x = b_{eq} \end{cases}$

Define states (x) necessary for LP optimization:

$p_{pv}(1:N) - Power\ from\ grid\ used\ from\ time\ step\ 1\ to\ N$

$p_{batt}(1:N) - Power\ from\ battery$

$E_{batt}(1:N) - Energy\ stored\ in\ batter$

$$x = [p_{pv}(1:N)\ \ p_{batt}(1:N)\ E_{batt}(1:N)]^T$$

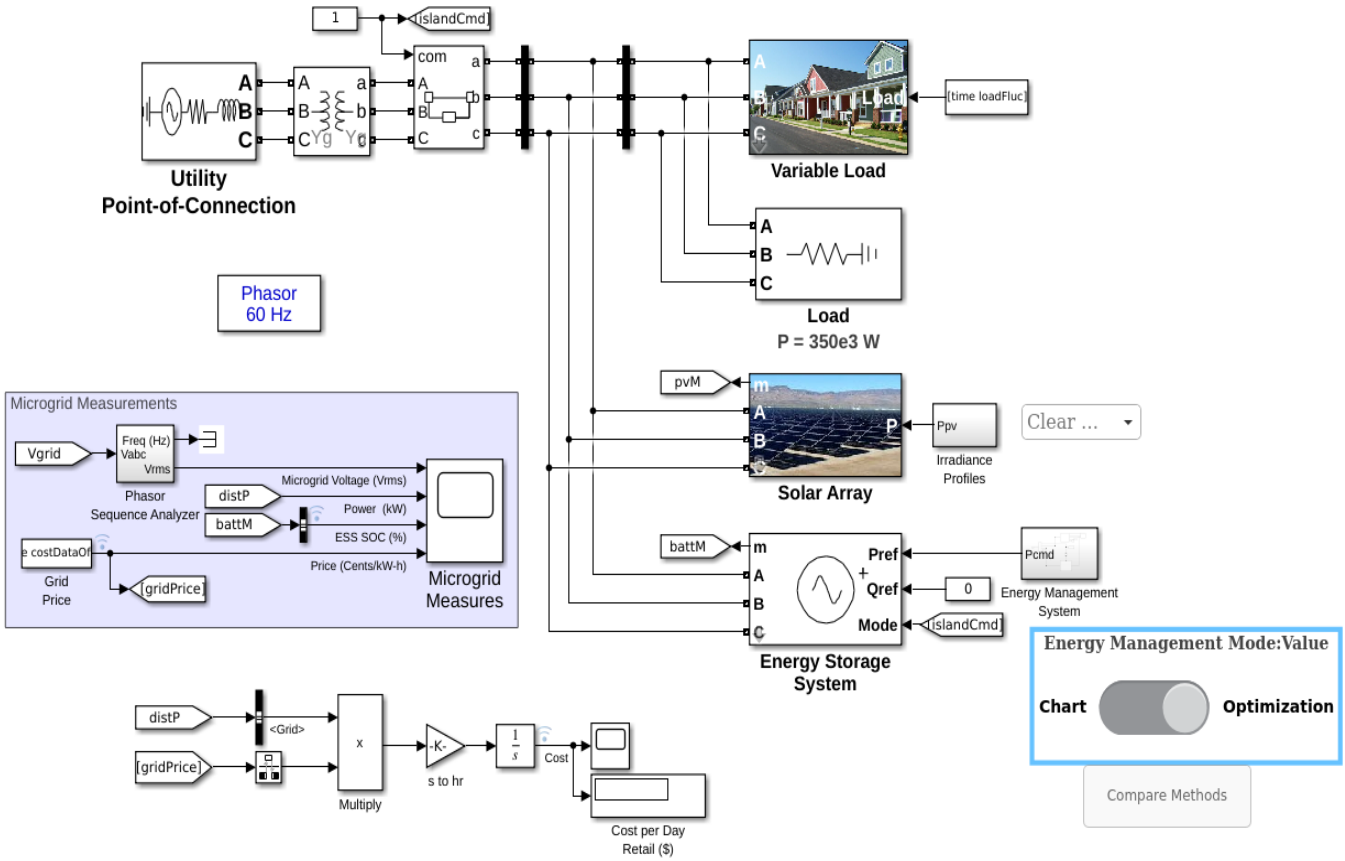

Figure 21. MATLAB Model for optimizing energy storage system

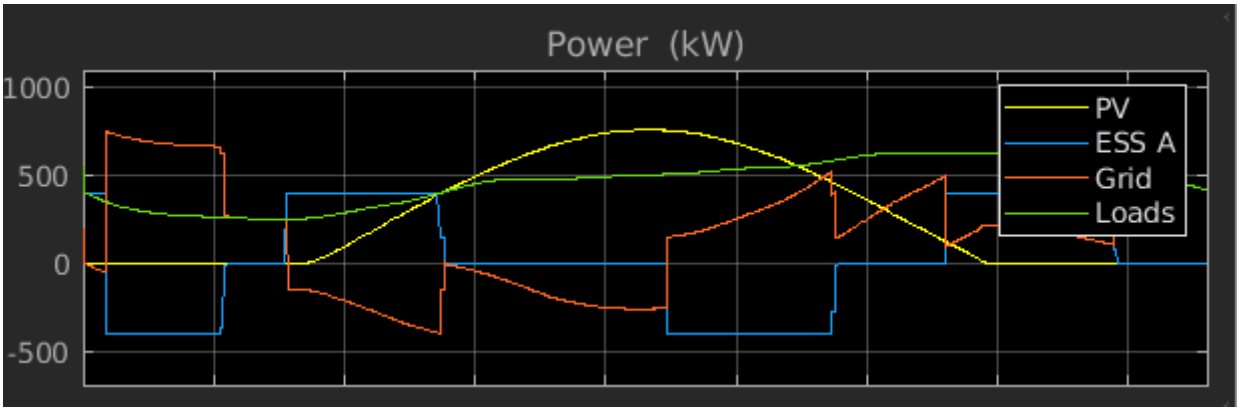

Figure 22. MATLAB Results

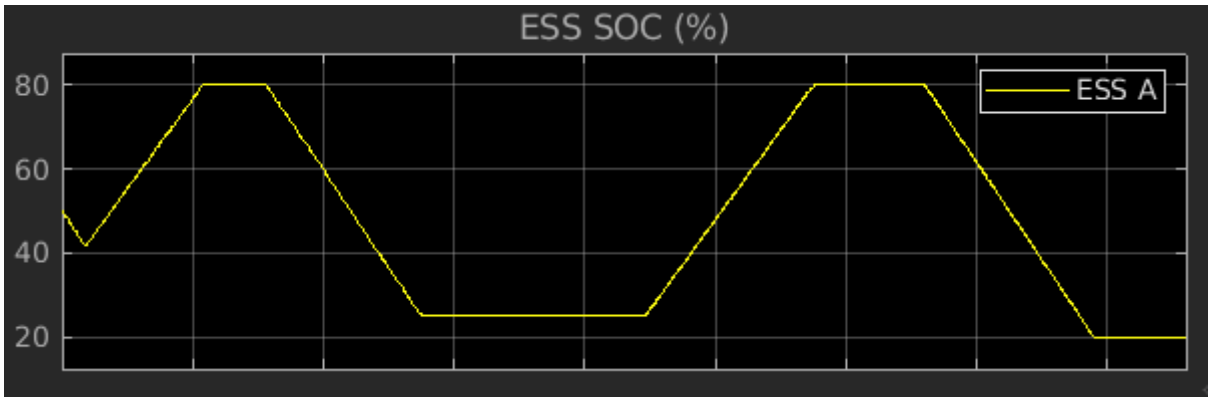

Figure 23. The optimized energy storage system

X. Conclusion

One of the main conclusions found during the sizing of three systems is an excess of energy production in summer and springtimes in the studied location. Excess energy production in summer was due to solar PV modules found in spring due to WTGs.

This means that optimal sizing methodologies have managed to sustain the balance of generation throughout the year. Therefore, producing an excess generation at certain times of the year due to the natural response of the renewable resources in the studied location towards the meteorological conditions. Consequently, this excess energy produced can be fully utilized in an energy storage element in the proposed system that will be the hydrogen tanks. Hydrogen tanks can then be used as the infrastructure for hydrogen refueling stations for the city. Not only will these stations utilize the excess energy produced, but they will also introduce power to gas concepts in the automotive industry, making the studied system an exemplar model for an energy hub for electricity and fuel production.

The second conclusion to be found from comparing the three energy systems is that the best configuration was a Solar PV/wind hybrid system with high penetration of solar PV. This configuration leads to the highest energy production with the minimum Levelized cost of energy. However, HOMER software preferred wind energy penetration rather than solar energy, evident in the hybrid mix of wind and PV modules. HOMER results were giving higher values of energy production (overestimated design) than the deterministic method, and these values were found to be exceeding the demand by almost 200%, which is not acceptable in terms of the design concepts, given that the HOMER and DBM were having the same input data (weather data and load profile).

References

[1] A.Emad, M. EL-Shimy & G. Amer, Sustainable Energy Technologies and Systems, ISBN: 978-620-2-05640-3 Book, Chapter 7, A Generalized Approach for Sizing of Single Source Variable Renewable Energy Systems with Storage

[2] Rehman, S., Al-Hadhrami, L. M., & Alam, M. M. (2015). Pumped hydro energy storage system: A technological review. Renewable and Sustainable Energy Reviews, 44, 586-598.

[3] Veldhuis, I. J. S., Richardson, R. N., & Stone, H. B. J. (2007). Hydrogen fuel in a marine environment. International Journal of Hydrogen Energy, 32(13), 2553-2566.

[4] Gelma Boneya, Design of a photovoltaic-Wind Hybrid Power Generation System for Ethiopian Remote area, Ph.D. thesis, Institue of Technology Department of Electrical and Computer Engineering, Addis Ababa University, 2011.

[5] Ghenai, C., Salameh, T., & Merabet, A. (2018). Technico-economic analysis of off grid solar PV/Fuel cell energy system for residential community in desert region. International Journal of Hydrogen Energy.

[6] M. Farrokhabadi, S. König, C. A. Cañizares, K. Bhattacharya and T. Leibfried, "Battery energy storage system models for microgrid stability analysis and dynamic simulation." IEEE Transactions on Power Systems, vol. 33, no. 2, pp. 2301-2312, 2017.

[7] M. N. Hussain and V. Agarwal, "A novel feedforward stabilizing technique to damp power oscillations caused by DC-DC converters fed from a DC bus." IEEE Journal of Emerging and Selected Topics in Power Electronics, vol. 8, no. 2, pp. 1528-1535, 2019.

[8] H. Wu, J. Wang, T. Liu, T. Yang and Y. Xing, "Modified SVPWM-controlled three-port three-phase AC–DC converters with reduced power conversion stages for wide voltage range applications," IEEE Transactions on Power Electronics, vol. 33, no. 8, pp. 6672-6686, 2017.

[9] J. Zhao and F. Dorfler, "Distributed control and optimization in DC microgrids," ELSEVIER, Automatica 61 2015): 18-26.

[10] Bukar, A. L., & Tan, C. W. (2019). A review on standalone photovoltaic-wind energy system with fuel cell: system optimization and energy management strategy. Journal of cleaner production..

[11] Mohamed, E. S. (2015). Dynamic Security of Interconnected Electric Power Systems-Volume 2: Dynamics and stability of conventional and renewable energy systems. LAP LAMBERT Academic Publishing.

[12] Skoplaki, E., & Palyvos, J. A. (2009). On the temperature dependence of photovoltaic module electrical performance: A review of efficiency/power correlations. Solar energy, 83(5), 614-624.

[13] Khiareddine, A., Salah, C. B., Rekioua, D., &Mimouni, M. F. (2018). Sizing methodology for hybrid photovoltaic/wind/hydrogen/battery integrated to energy management strategy for pumping system. Energy, 153, 743-762.

[14] Larminie, J., A. Dicks, and M.S. McDonald, Fuel cell systems explained. Vol. 2. 2003: J. Wiley Chichester, UK.

[15] Fathy, A. (2016). A reliable methodology based on mine blast optimization algorithm for optimal sizing of hybrid PV-wind-FC system for remote area in Egypt. Renewable energy, 95, 367-380.

[16]https://openei.org/datasets/files/961/pub/RESIDENTIAL_LOAD_DATA_E_PLUS_OUTPUT/BASE/

[17] Meteonorm software platform, available online on https://meteonorm.com/en/ Accessed Apr 1, 2019

[18] IRENA (2018), Renewable Power Generation Costs in 2017, International Renewable Energy Agency, Abu Dhabi.

[19] HOMER software program, available online on https://www.homerenergy.com/ Accessed Apr 1, 2019

Appendix A Software Tools

A.1 METEONORM Model

Figure A.1 METEONORM software

A.2 HOMER Model

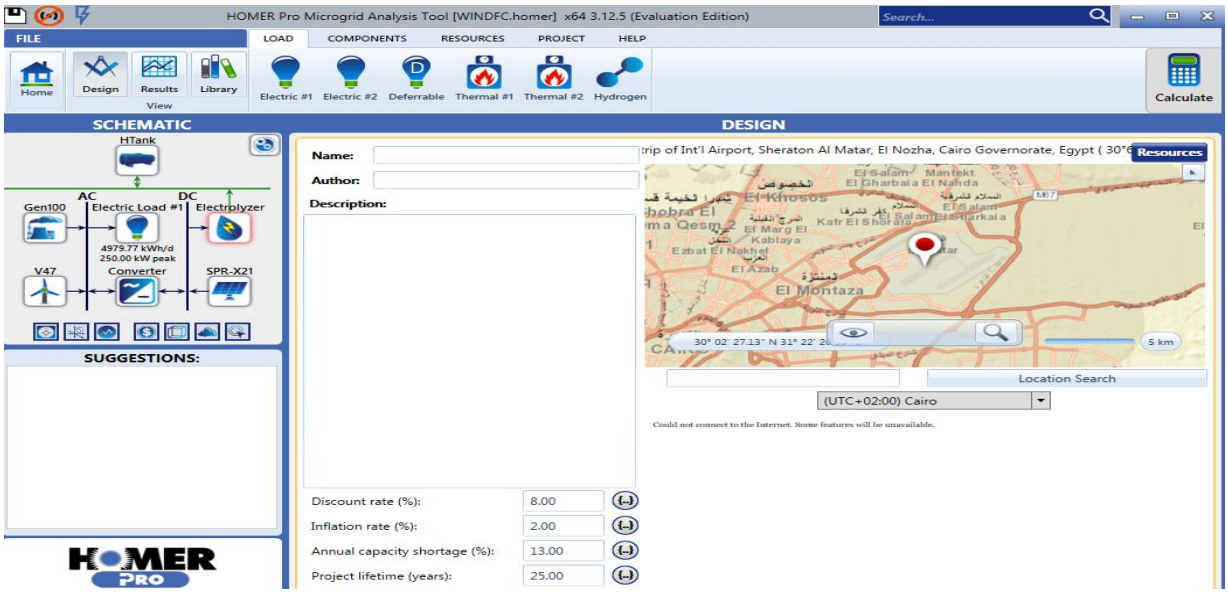

Figure A.2.1 HOMER Configuration

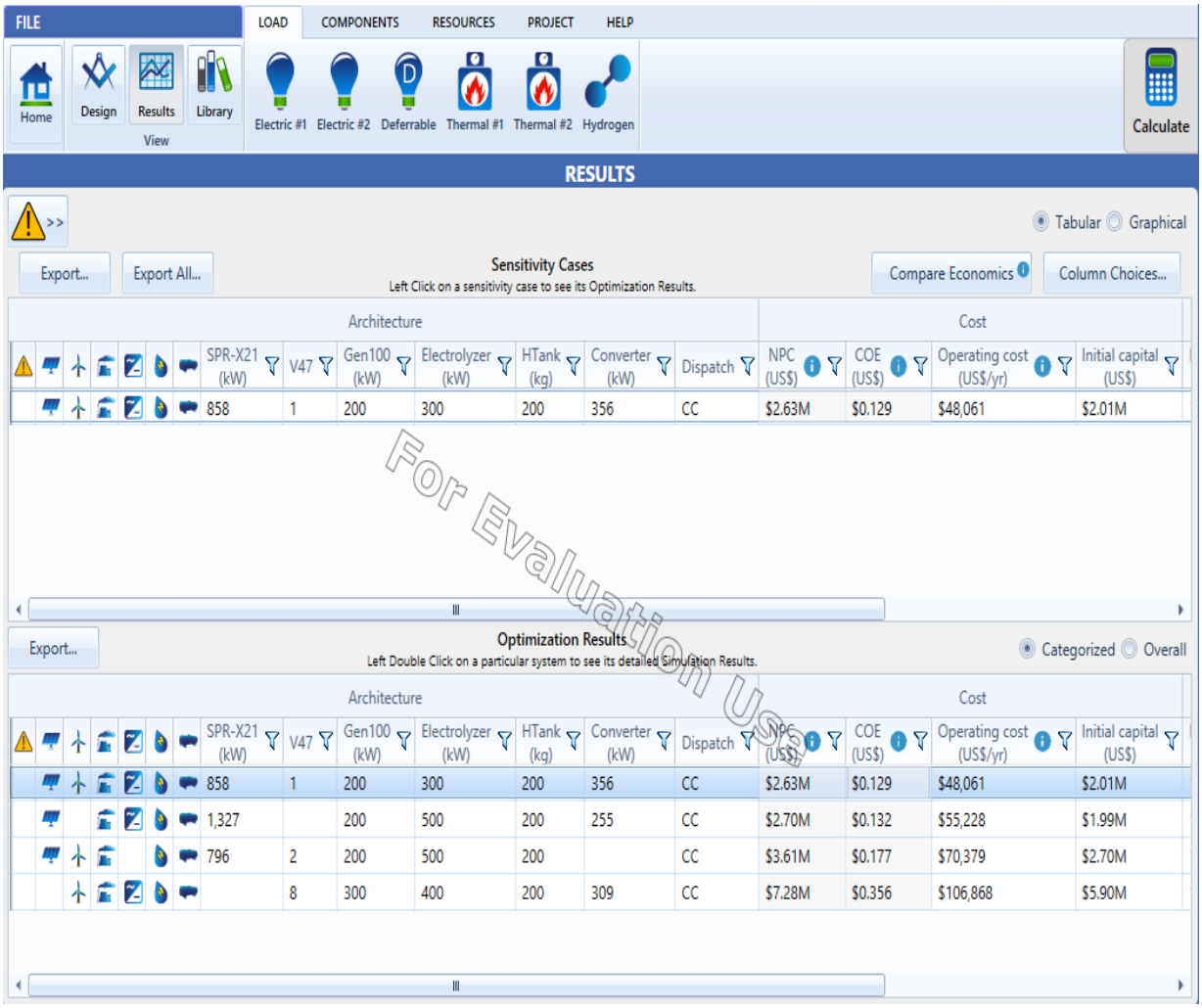

Figure A.2.2 HOMER Results

A.3 SAM MODEL

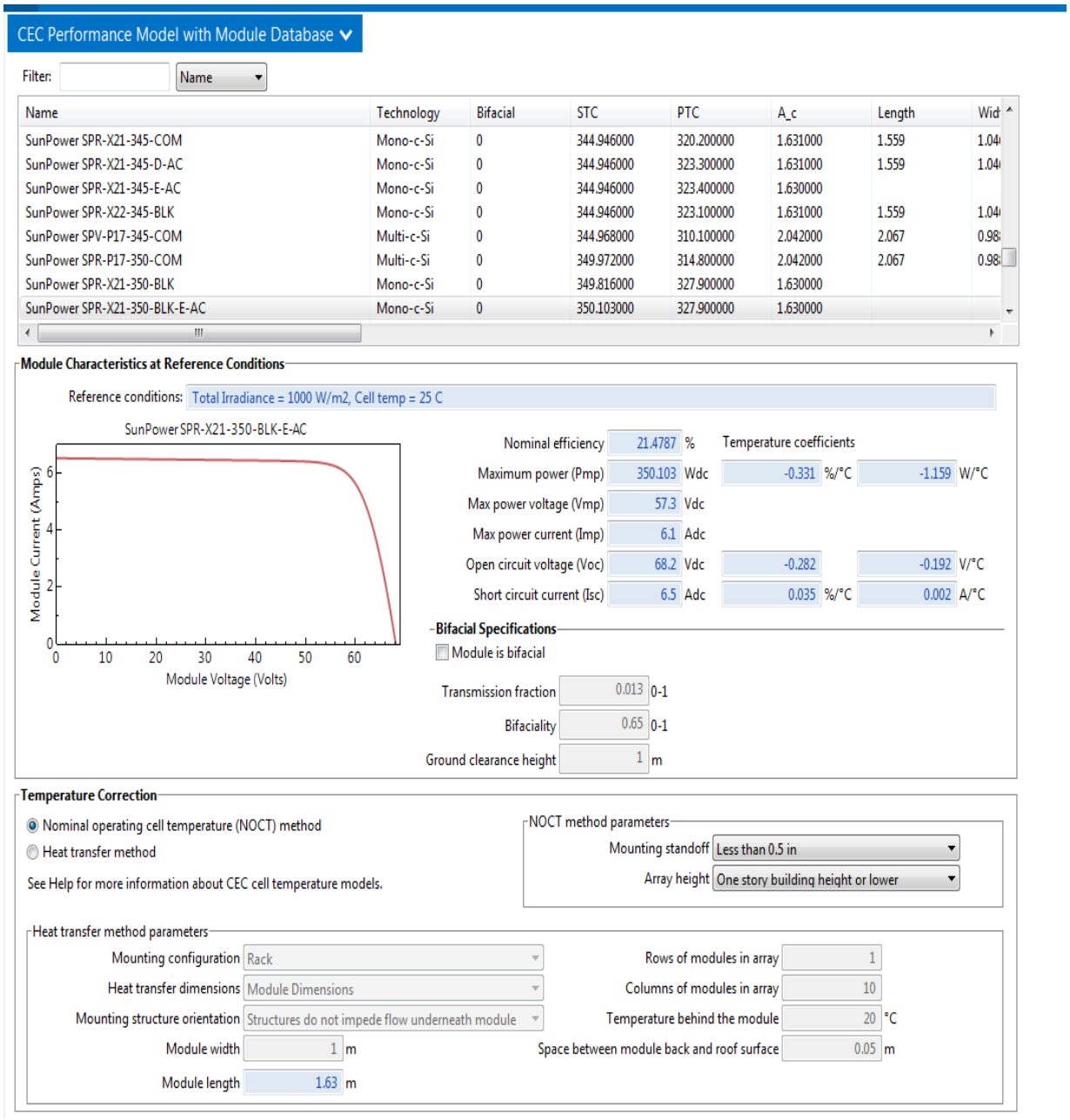

Figure A.3.1 SAM Solar PV Configuration

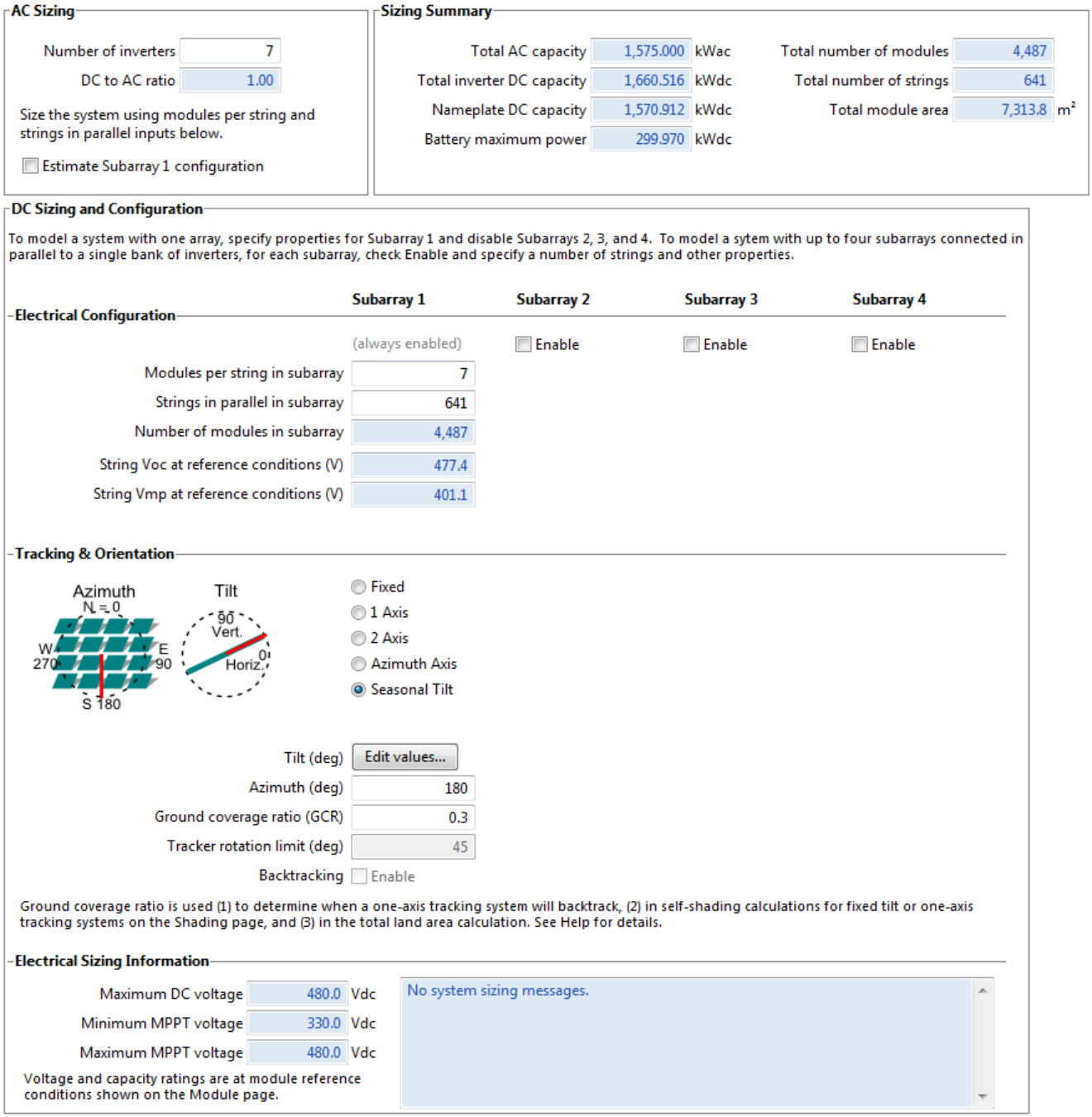

Figure A.3.2 System Configuration

Code Appendix:

```
function [Pgrid,Pbatt,Ebatt] = battSolarOptimize(N,dt,Ppv,Pload,Einit,Cost,FinalWeight,batteryMinMax)

% Minimize the cost of power from the grid while meeting load with power
% from PV, battery and grid

prob = optimproblem;

% Decision variables
PgridV = optimvar('PgridV',N);
PbattV = optimvar('PbattV',N,'LowerBound',batteryMinMax.Pmin,'UpperBound',batteryMinMax.Pmax);
EbattV = optimvar('EbattV',N,'LowerBound',batteryMinMax.Emin,'UpperBound',batteryMinMax.Emax);
% Minimize cost of electricity from the grid
prob.ObjectiveSense = 'minimize';
prob.Objective = dt*Cost'*PgridV - FinalWeight*EbattV(N);

% Power input/output to battery
prob.Constraints.energyBalance = optimconstr(N);
prob.Constraints.energyBalance(1) = EbattV(1) == Einit;
prob.Constraints.energyBalance(2:N) = EbattV(2:N) == EbattV(1:N-1) - PbattV(1:N-1)*dt;

% Satisfy power load with power from PV, grid and battery
prob.Constraints.loadBalance = Ppv + PgridV + PbattV == Pload;

% Solve the linear program
options = optimoptions(prob.optimoptions,'Display','none');
[values,~,exitflag] = solve(prob,'Options',options);

% Parse optmization results
if exitflag <= 0
    Pgrid = zeros(N,1);
    Pbatt = zeros(N,1);
    Ebatt = zeros(N,1);
else
    Pgrid = values.PgridV;
    Pbatt = values.PbattV;
    Ebatt = values.EbattV;
end
```

```
% Load Power Data from Existing PV array
load pvLoadPriceData;

% Set up Optimization Parameters
numDays = 1;            % Number of consecutive days
FinalWeight = 1;      % Final weight on energy storage
timeOptimize = 5;       % Time step for optimization [min]

% Battery/PV parameters
panelArea = 2500;
panelEff = 0.3;

battEnergy = 2500*3.6e6;
Einit = 0.5*battEnergy;
batteryMinMax.Emax = 0.8*battEnergy;
batteryMinMax.Emin = 0.2*battEnergy;
batteryMinMax.Pmin = -400e3;
batteryMinMax.Pmax = 400e3;

% Rescale data to align with desired time steps
stepAdjust = (timeOptimize*60)/(time(2)-time(1));
cloudyPpv = panelArea*panelEff*repmat(cloudyDay(2:stepAdjust:end),numDays,1);
clearPpv = panelArea*panelEff*repmat(clearDay(2:stepAdjust:end),numDays,1);

% Adjust and Select Loading
loadSelect = 3;
loadBase = 350e3;
loadFluc = repmat(loadData(2:stepAdjust:end,loadSelect),numDays,1) + loadBase;

% Grid Price Values [$/kWh]
C = repmat(costData(2:stepAdjust:end),numDays,1);

% Select Desired Data for Optimization
Ppv = clearPpv;
% Ppv = cloudyPpv;
Pload = loadFluc;
```

```
% Setup Time Vectors
dt = timeOptimize*60;
N = numDays*(numel(time(1:stepAdjust:end))-1);
tvec = (1:N)'*dt;

% Optimize Grid Energy Usage
[Pgrid,Pbatt,Ebatt] = battSolarOptimize(N,dt,Ppv,Pload,Einit,C,FinalWeight,batteryMinMax);

% Plot Results
figure;
subplot(3,1,1);
thour = tvec/3600;
plot(thour,Ebatt/3.6e6); grid on;
xlabel('Time [hrs]'); ylabel('Battery Energy [kW-h]');

subplot(3,1,2);
plot(thour,C); grid on;
xlabel('Time [hrs]'); ylabel('Grid Price [$/kWh]');

subplot(3,1,3);
plot(thour,Ppv/1e3,thour,Pbatt/1e3,thour,Pgrid/1e3,thour,Pload/1e3);
grid on;
legend('PV','Battery','Grid','Load')
xlabel('Time [hrs]'); ylabel('Power [W]');
```

```
load pvLoadPriceData.mat;
costDataOffset = costData + 5;

% Microgrid Settings
panelArea = 2500;   % Area of PV Array [m^2]
panelEff = 0.3;     % Efficiency of Array
loadBase = 350e3;   % Base Load of Microgrid [W]

BattCap = 2500;     % Energy Storage Rated Capacity [kWh]
batteryMinMax.Pmin = -400e3;    % Max Discharge Rate [W]
batteryMinMax.Pmax = 400e3;     % Max Charge Rate [W]

% Online optimization parameters
FinalWeight = 1;    % Final weight on energy storage
timeOptimize = 5;    % Time step for optimization [min]
timePred = 20;        % Predict ahead horizon [hours]

% Compute PV Array Power Output
cloudyPpv = panelArea*panelEff*cloudyDay;
clearPpv = panelArea*panelEff*clearDay;

% Select Load Profile
loadSelect = 3;
loadFluc = loadData(:,loadSelect);

% Battery SOC Energy constraints (keep between 20%-80% SOC)
battEnergy = 3.6e6*BattCap;
batteryMinMax.Emax = 0.8*battEnergy;
batteryMinMax.Emin = 0.2*battEnergy;

% Setup Optimization time vector
optTime = timeOptimize*60;
stepAdjust = (timeOptimize*60)/(time(2)-time(1));
N = numel(time(1:stepAdjust:end))-1;
tvec = (1:N)'*optTime;

% Horizon for "sliding" optimization
M = find(tvec > timePred*3600,1,'first');
```